NATIONAL INSTITUTE FOR FUSION SCIENCE

Secondary Charged Particle Emission from
Proton Conductive Oxides by Ion Impact

N. Matsunami, E. Hatanaka, J. Kondoh, H. Hosaka,
K. Tsumori, H. Sakaue and H. Tawara

RESEARCH REPORT
NIFS-DATA Series

TOKI, JAPAN

Secondary charged particle emission from proton conductive oxides by ion impact

Noriaki Matsunami, E. Hatanaka, J. Kondoh, H. Hosaka[*],
K. Tsumori[*], H. Sakaue[*] and H. Tawara[*]

Energy Engineering and Science, Engineering, Nagoya University
Furo-Cho, Chikusa-ku, Nagoya 464-8603, Japan
[*]National Institute for Fusion Science, Toki 509-5259, Japan

Abstract

Secondary charged particle emission (SCPE) from a proton conductive perovskite oxide, namely, $SrCe_{0.95}Yb_{0.05}O_{3-\delta}$ (SCO) film on Si by ion impact was measured using a charge collector method. When the ion projected range is much longer than the film thickness, the SCPE yields are found to be nearly independent of the ion beam current (I_B) for I_B < a few nA, giving the SCPE yields under charge-accumulation free condition, to contrast with the results for the thick polycrystalline SCO which shows a strong dependence of the SCPE yields on the ion beam current. Several corrections are required to evaluate the secondary positive ion yields and a method is described.

Key words: secondary electron, secondary ion, proton conductive oxides, ion impact

1. Introduction

Neutral atoms and charged particles such as secondary electrons and ions are emitted from solid surfaces by ion impact. There are few investigations of the secondary charged particle emission (SCPE) from functional oxide surfaces such as ionic conductive oxides, high temperature superconductor oxides and so on, comparing with extensive studies on metallic surfaces [1-3]. Investigations of secondary electron emission (SEE) and secondary positive ion emission (SPIE) from these materials may be of interest in both fundamental aspects of ion-solid interactions, e.g., comparison with SPIE from oxygen covered metals or metal oxides, and applications, e.g., SEE for ion beam current monitor and SPIE for quantitative secondary ion mass spectroscopy (SIMS). In these materials, the surface potential during ion impact may not be zero due to charge accumulation on their surfaces, because of high resistivity or lack of sufficient free carriers. This often results in difficulty to obtain the well-defined SCPE yield. In the previous work [4], we have reported a strong dependence of the SCPE yield on the ion beam current for the thick polycrystalline (p-) $SrCe_{0.95}Yb_{0.05}O_{3-\delta}$ (abbreviated as SCO herein) target, which is known as a proton conductive oxide at high temperature (> 600 °C) in the presence of H_2 or water [5]. Use of a thin film of these materials on a conductive substrate may reduce the charge accumulation problem to give the well-defined SCPE yields.

In this paper, we report the well-defined SEE yields from thin SCO film on Si substrate obtained with current measurements using a cylindrical Faraday cup. We find that the SEE yields are independent of the ion beam current (I_B) for I_B < a few nA, when the ion projected range (R_p) is much longer than the film thickness (d) and that the SEE yields depend very slightly on ion beam current when R_p is much shorter than d. We have also measured positive currents using a negatively biased Faraday cup. A method is described to evaluate the secondary positive ion yield from this measurement. Information of SCPE yields of non-metallic oxide surfaces is important for understanding of plasma-wall interactions.

2. Experimental

The experimental methods used in this study are the same as those described in refs. [4,6]. Ion beams with the energy of 20 to 100 keV (higher energy experiments) were obtained using a 200 kV Cockroft type accelerator at Nagoya University [6]. Beams of 1mm in diameter were led to the SCPE measurement assembly shown in Fig. 1. The incidence angle was normal to the target surface. The electrical currents of the secondary charged particles were measured with a cylindrical cup of stainless steel surrounded by a shield. Positive or negative bias can be applied to either the target or cup, while the non-biased cup or target was grounded, and the shield was grounded. The base

pressure of the target chamber was 3×10^{-8} Torr and the pressure during SCPE measurement was ~10^{-7} Torr. The measurements were done at room temperature. The target surface was uncleaned in the higher energy experiments.

Ion beams with lower energies (≤ 2.5 keV) were obtained with a compact duo-plasmatron at National Institute for Fusion Science [4] and the SCPE measurement system is similar to that described above. The vacuum of the target chamber was 1×10^{-10} Torr. The target surface can be cleaned using ion sputtering technique and the surface impurities were examined by Auger electron spectroscopy.

Let I_T and I_C be the currents of the target and the Faraday cup, then the SEE yield (Y^- or γ_e) and SPIE yield Y^+ are given by

$$Y^- = -I_C /(I_T + I_C) \text{ for } I_C < 0 \quad \text{and}$$
$$Y^+ = I_C /(I_T + I_C) \text{ for } I_C > 0. \quad (1)$$

$I_T + I_C = I_B$ is the ion beam current. Here the secondary negative ion yield is assumed to be much smaller than the SEE yield. As discussed later (see Fig. 1(b)), corrections are required to obtain the true SPIE yield (γ^+) from Y^+.

SCO film was deposited on Si at 740 °C using a pulsed ArF-excimer-laser (193nm) deposition (PLD) method [7]. Thickness and composition of the film were examined by means of He Rutherford backscattering spectroscopy (RBS) using a Van de Graaff accelerator at Nagoya University. The thickness is 100 and 280 nm for higher and lower energy experiments. The composition was closely stoichiometric, except that an O-rich SrO_2 layer of 60 and 100 nm was found between the SCO film and Si interface for 100 and 280 nm films, respectively, and this layer seems to act as a buffer layer for the SCO film growth. Proton induced X-ray analysis shows no detectable impurities.

3. Results and Discussion
3.1 Ion beam current dependence of SCPE yield

It has been reported previously [4] that for the thick p-SCO sample, SCPE yield depends strongly on the ion beam current (I_B). Firstly, dependence on I_B was investigated for the SCO film on Si. The results are shown in Figs. 2 and 3 for 100 keV H^+ and 20 keV Ar^+, respectively. To contrast with the thick p-SCO results, SCPE yields from the SCO film on Si for 100 keV H^+ or 20 keV Ar^+ are found to be constant or nearly constant for 10 pA to a few nA. I_B-dependence observed for lower currents ($< \sim 10$ pA) is partly due to background current. For such low currents, a very careful correction is required

and thus no further discussion is made hereafter.

Depending on positive bias, decrease of SEE yields is seen at large currents. This can be caused by charge accumulation effects: SEE yields are determined by a dynamic balance between the charge left at target surface by SEE (surface charge accumulation) and/or charge carried by ions in the film (interior charge accumulation) and compensation of these charges by electrons generated by ion impact in the film and/or the conductive substrate. Surface charge accumulation is considered to be similar for 100 keV H^+ and 20 keV Ar^+, since SEE yields are similar for both cases. For 100 keV H^+ impact, whose projected range (571 nm) is much longer than the film thickness, there is no appreciable interior charge accumulation, while for 20 keV Ar^+ impact, whose projected range (16 nm) is much shorter than the film thickness, there may be interior charge accumulation. There is no compensation from the substrate for 20 keV Ar^+ impact. These differences could be a reason for a slight different I_B-dependence of SEE yields and difference of the bias dependence of SEE yields (SEE with negative bias is seen in Fig. 2(a) for 100 keV H^+) between these two ions. Information of the carrier concentration and mobility in the SCO film under ion impact is necessary for detail evaluation of the charge accumulation effects. In this paper, the charge accumulation effects are not discussed further but instead we concentrate on SCPE yields under charge-accumulation free conditions or I_B-independent SCPE yields.

It also appears that SEE and SPIE yields reach their maxima at the bias of ± 90V, meaning that +90 V is adequate to suppress a flow of secondary positive ions from the target to the collector, keep tertiary electrons in the collector cup, and -90 V is adequate to suppress SEE, as discussed in [1]. This is depicted more clearly in Fig. 4 for 100 keV H^+. It is also found that in the lower energy experiments, the SCPE yields of uncleaned SCO surface are nearly the same as those of cleaned SCO surface (see Tables 1 and 2), as reported previously for the p-SCO. Generally, the bias was applied to the Faraday cup and zero bias on the sample. For higher energy experiments, it is mentioned that positive (negative) bias on the Faraday cup with zero bias on the sample and zero bias on the cup with negative (positive) bias on the sample give the same SCPE yield, within 10%.

3.2 SEE yield

SEE yields (γ_e) for H^+ and Ar^+ which were taken at I_B-independent or nearly I_B-independent region and at bias of +90 V, are summarized in

Table 1. It appears that γ_e is nearly proportional to the electronic stopping power (S_e) and that the proportionality constants are nearly the same for H^+ and Ar^+. The proportionality constants for the SCO films are comparable with those of metallic oxides and are larger by a factor of 2~3 than those of metals [1,4]. The results for molecular hydrogen ion impact are included. The SEE yields for molecular hydrogen are given as those per nucleon. Notice that considerable molecular effect was observed. The SEE yields of the SCO films are comparable with those of the p-SCO at low ion beam current, where charge accumulation effects are minimized [4].

3.3 SPIE yield

As discussed in ref. [4], the backscattered ions and atoms, and sputtered atoms hit the Faraday cup collector and generate tertiary electrons which leave the negatively biased collector, generating a positive current, as shown in Fig. 1(b). Thus, these contributions (Y_C) should be subtracted from Y^+ to obtain the true γ^+.

A method to estimate Y_C, which is described elsewhere in detail [4,8], is briefly mentioned here. Firstly, the yield of backscattered ions and atoms, $Y_B(E, \theta)$ per incident ion, and that of sputtered atoms and ions, $Y_S(E, \theta)$ are calculated as functions of the exit energy E and exit angle θ measured from the surface normal, using simulation such as TRIM97 [9] and TRVMC95 [10]. An obvious contribution to Y_C is backscattered positive ions, Y_B^+. With the positive fraction $f_B^+(E, \theta)$, Y_B^+ is given by

$$Y_B^+ = \iint f_B^+(E, \theta)Y_B(E, \theta) \, dE \, d\theta . (2)$$

The data of $f^+(E, \theta)$ is scarce [11-15], so we adopt a simple form,

$$f_B^+(E, \theta) = P_0 \exp(-P_1/(E_\perp)^{1/2}), \qquad (3)$$

where P_0 and P_1 are constants and $E_\perp = E(\cos(\theta))^2$. P_0 and P_1 are 0.6 and 1.9 for H^+, 0.23 and 1.47 for Ar^+, and 0.9 and 8.15 for C^+, N^+. $f_B^+(E, \theta)$ is shown graphically as a function of $E_\perp$ for H^+, Ar^+, C^+ and N^+ in Fig. 5. Charge fraction of O is approximated by that of C and N.

Contributions to Y_C from positive currents caused by SEE from Faraday cup collector under impact of these backscattered and sputtered atoms (and ions), Y_{BK} and Y_{SK} are given by

$$Y_{BK} = \iint Y_B(E, \theta) \gamma_{eKC}(E) / \cos(\theta) \, dE \, d\theta , (4)$$

$$Y_{SK} = \iint Y_S(E, \theta) \gamma_{eKC}(E) / \cos(\theta) \, dE \, d\theta . (5)$$

$\gamma_{eKC}(E)$ is the kinetic emission contribution of the SEE yields from the collector and $1 / \cos(\theta)$ dependence is assumed. Available data [16] of $\gamma_{eKC}(E)$ for Ar^+, H^+ and O^+ are shown in Fig. 6 and fitted by the following formula,

$$\ln(\gamma_{eKC}(E)) = \Sigma \, C_n \ln(E)^n, \, n=0-3. \quad (6)$$

Constants (C_0, C_1, C_2, C_3) are (-1.463, 1.598, -3.9, 0.03562), (-2.553, 2.12, -0.4208, 0.03533) and (-0.2335, 0.6768, -0.07027, 0.01131) for H^+, Ar^+ and O^+, respectively. Independence of $\gamma_{eKC}(E)$ on the charge state of these ions and atoms is also assumed. $\gamma_{eKC}(E)$ for Ce and Sr are taken as constant (K) times $\gamma_{eKC}(E)$ for Ar and the constant K is determined as 0.743 and 0.553, respectively, considering that the kinetic emission is proportional to the electronic stopping power. Similarly, the potential emission contributions, Y_{BP} and Y_{SP} are given by

$$Y_{BP} = \gamma_{ePC} \iint f_B^+(E, \theta)Y_B(E, \theta) \, dE \, d\theta , (7)$$

$$Y_{SP} = \gamma_{ePC} \iint f_S^+(E, \theta)Y_S(E, \theta) \, dE \, d\theta . (8)$$

γ_{ePC} is the potential emission contribution of the SEE yields due to backscattered and sputtered ions. γ_{ePC} for Ar^+ and H^+ are approximated by the experimental values for Cu, ie., 0.1 and 0.07, respectively, taking into account that stainless steel has similar work function and Fermi energy to Cu. γ_{ePC} for O^+ is taken as 0.07, since the ionization potential of O is close to that of H.

Y^+ and Y_c are given in Table 2. Backscattered yield Y_B and sputtering yield Y_S, which are the average calculated with TRIM97 [9] and TRVMC95 [10] are also given. Notice that Y_c has considerable contribution to Y^+. For H^+, Y_B^+ has a major contribution and for Ar^+, Y_{SK} has a major contribution. Accuracy of simulation is also crucial, because sometimes, two simulation give values different by a factor of 2-3. As seen in Table 2, γ^+/Y_S is larger than unity for H^+ and is not constant for Ar^+. However, considering accuracy of quantities used in this study, values of Y_c are tolerable. It could be improved, if quantities required for Y_c evaluation such as charged fraction were accurately measured

4. Summary

We have measured secondary charged particle emission yields from SCO films on Si. It is found that the SCPE yield is nearly constant, over a wide range of ion beam current, as contrast with a strong current dependent SCPE for the thick poly-

crystalline SCO. The current independent SCPE indicate insignificant charge-up problem. The SEE yields are found to be nearly proportional to the electronic stopping power and the proportionality constants are comparable with those of metallic oxides. We also estimated the corrections for positive ion yields involved in Faraday-cup current measurement. Various quantities such as charged fraction should be more accurately known to estimate these corrections.

References
1. G. Hohler (Ed.), Particle Induced Electron Emission I and II, Springer, Berlin, 1991.
2. A. Benninghoven, Surf. Sci. 53(1975)596.
3. M. L. Yu, Sputtering by Particle Bombardment III, ed. R. Behrisch and K. Wittmaack (Springer-Verlag, 1991)chap.3.
4. K. Hosaka, N. Matsunami and H. Tawara, Nucl. Instr. & Meth. B149(1999)414.
5. H. Iwahara, T. Esaka, H. Uchida and N. Maeda, Solid State Ionics 3-4, (1981)359.
6. N. Matsunami, S. Majima and T. Kawamura, Nucl. Instr. & Meth. B135(1998)450.
7. N. Sata, H. Matsuta, Y. Akiyama, Y. Chiba, S. Shin and M. Ishigame, Solid State Ionics 97(1997)437.
8. E. Hatanaka, Thesis for B. D. (Nagoya university, 1998).
9. J. F. Ziegler, J. P. Biersack and U. Littmark, The Stopping and Ranges of Ions in Solids, Pergamon, 1985.
10. W. Eckstein, Computer Simulation of Ion-Solid interactions, Springer, 1991.
11. M. C. Cross, Phys. Rev. B15(1977)602.
12. S. H. Overbury, P.F. Dittner and S. Datz, Rad. Eff. 41(1979)219.
13. R. S. Bhattacharya, W. Eckstein and H. Verbeek, Surf. Sci. 93(1980)563.
14. S. B. Luitjens, A. J. Algra, E. P. Th. M. Suurmeijer and A. L. Boers, Surf. Sci. 99(1980)652.
15. W. F. S. Poehlman, R. S. Bhattacharya, and D. A. Thompson, Nucl. Instrum. Meth. 170(1980)549.
16. E. V. Alonso, R.A. Baragiola, J. Ferron and A. O.-Florio, Rad. Eff. 45(1979)119.

Table 1 SEE yields (γ_e) from SCO film on Si for Ar^+, H^+, H_2^+ and H_3^+ impact with energy E(keV). For H_2^+ and H_3^+ impact, γ_e is given as SEE yields per nucleon. The electronic stopping power and projected range calculated by TRIM are also included. The γ_e and γ_e/S_e in parentheses are for cleaned surfaces.

E(keV)	Ion	γ_e	S_e(eV/nm)	γ_e/S_e(nm/eV)	R_P(nm)
100	H^+	3.2	173	0.019	571
50	H^+	3.3	158	0.021	313
20	H^+	3.0	121	0.025	146
2.5	H^+	1.4 (1.4)	47.5	0.029(0.03)	24
1.0	H^+	0.88(1.1)	31.5	0.028(0.035)	11
100	H_2^+	2.8			
40	H_2^+	2.5			
20	H_2^+	1.6	88.7		81
60	H_3^+	2.0			
30	H_3^+	0.96			
21	H_3^+	0.92	75.5		59
150	Ar^+	8.0	590	0.014	94
100	Ar^+	8.2	481	0.017	64
50	Ar^+	6.0	340	0.018	34
20	Ar^+	4.2	215	0.02	16
2.5	Ar^+	1.1(1.7)	76.1	0.014(0.02)	3.7
1.0	Ar^+	0.55(0.83)	48.1	0.011(0.017)	2.2

Table 2 Y^+ and correction Y_c with backscattered yield Y_B sputtering yield Y_S, calculated with TRIM97[8] and TRVMC95[9]. $\gamma^+ = Y^+-Y_c$. S_e and S_n are the electronic and nuclear stopping powers(eV/nm). Results of a clean Cu and YBCO are included [4,6].

E (keV)	Ion	Sample	Y^+	Y_B	Y_S	Y_c	γ^+	S_e (eV/nm)	S_n
2.5	H^+	Cu	0.18	0.19	0.023	0.07	0.1	48.9	3.3
2.5	Ar^+	Cu	7.6E-4	0.057	4.2	6.8E-4	8E-5	69	779
2.5	H^+	SCO	0.11	0.18	8.6E-3	0.08	0.03	49.1	2.1
2.5	Ar^+	SCO	0.04	0.066	1.3	0.036	0.004	78	465
100	Ar^+	SCO	0.45	0.025	1.6	0.38	0.065	493	621
150	Ar^+	SCO	0.44	0.021	1.35	0.27	0.13	604	563
2.5	H^+	YBCO	0.18	0.12	0.015	0.05	0.13	51.4	2.5
30	Ar^+	YBCO	0.47	0.28	3.2	0.21	0.26	276	849
150	Ar^+	YBCO	0.7	0.016	2.5	0.32	0.38	504	748

Fig.1 (a) Schematics of positively biased Faraday-cup-collector for secondary electrons and (b) schematics of negatively biased Faraday-cup-collector for secondary positive ions, where backscattered ions and atoms (●) and sputtered atoms and ions (o) hit the collector, generating tertiary electrons emitted from the collector or positive currents to be subtracted to obtain true secondary positive ion yield.
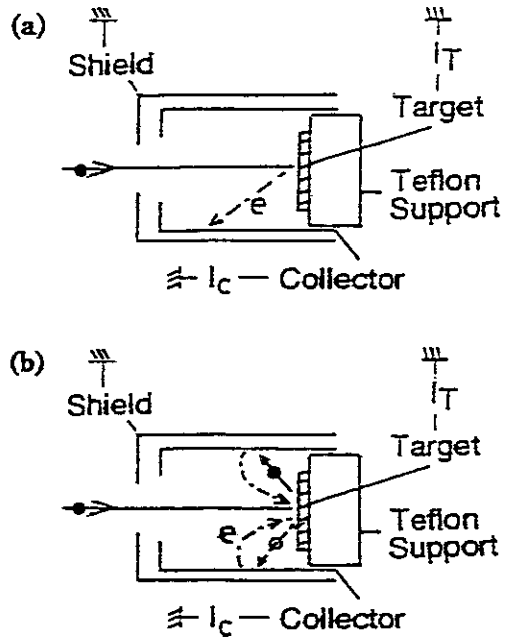

Fig. 2. (a) SEE from SCO film on Si by 100 keV H^+ ion for various bias voltage and (b) positive yield from SCO film on Si by 100 keV H^+ ion for various bias voltage.
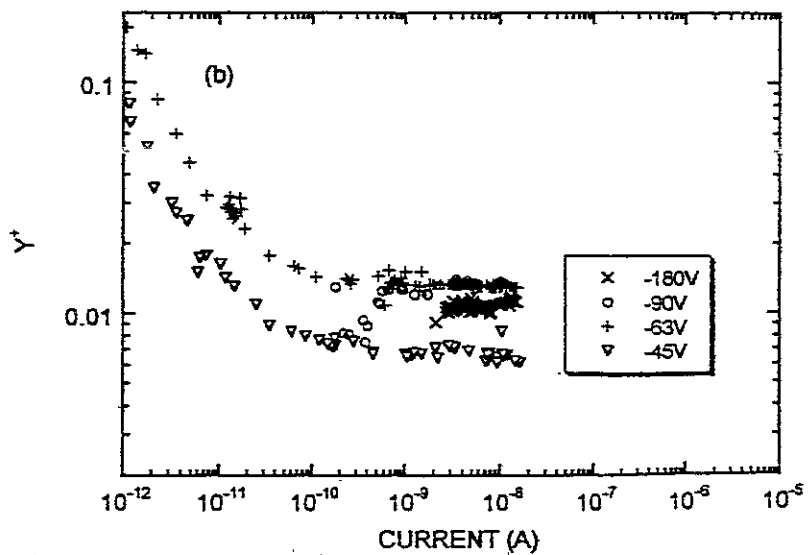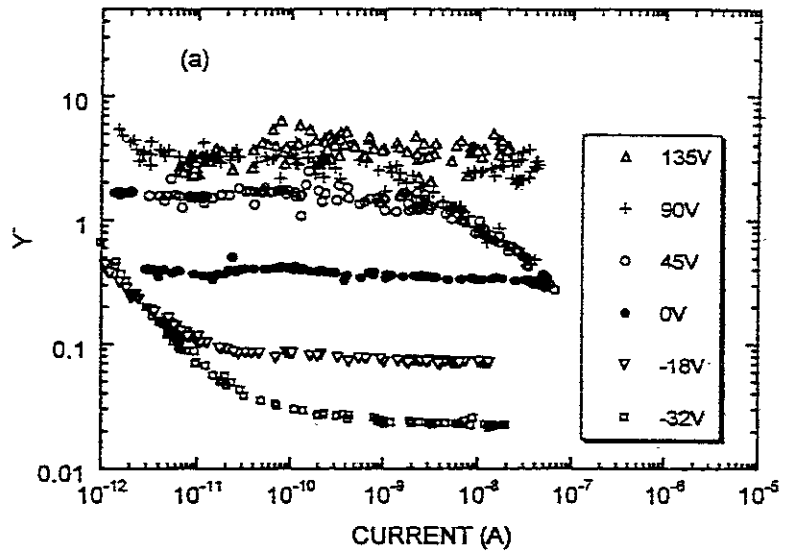
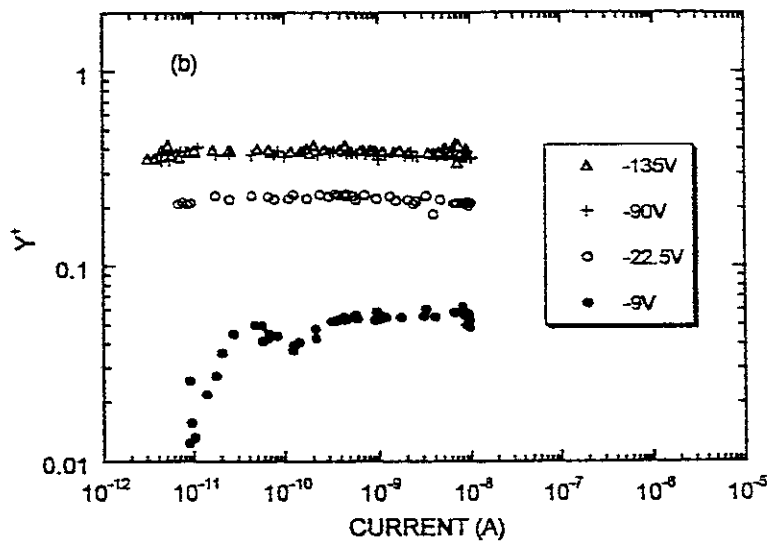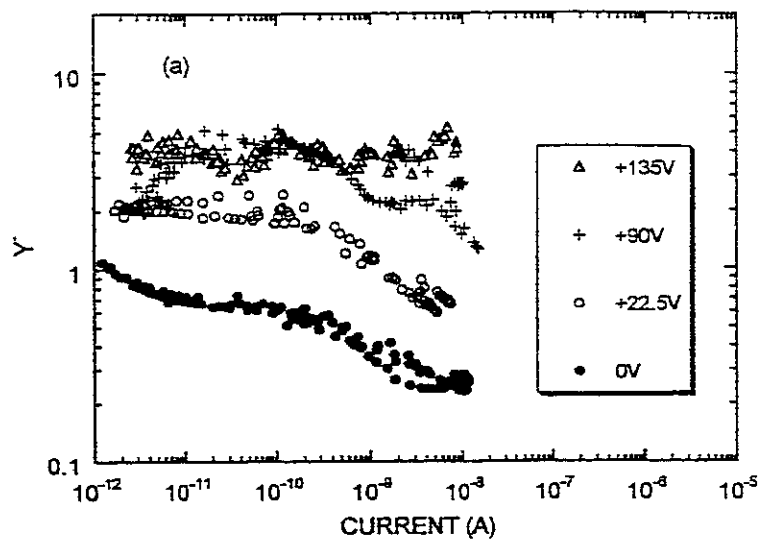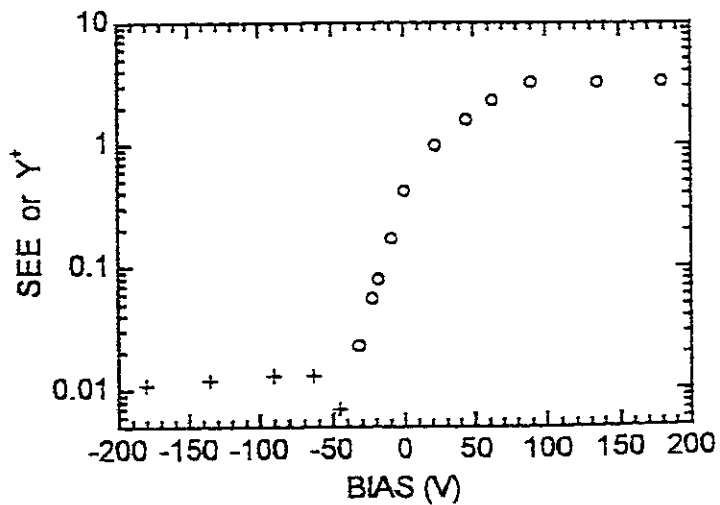Fig. 3. Similar to Fig. 2 except for 20 keV Ar$^+$ ion.

(a)

△	+135V
+	+90V
○	+22.5V
●	0V

Y

CURRENT (A)

(b)

△	-135V
+	-90V
○	-22.5V
●	-9V

Y$^+$

CURRENT (A)

Fig. 4 SEE (o) and Y$^+$ (+) vs Faraday cup bias for 100 keV H$^+$ ion.
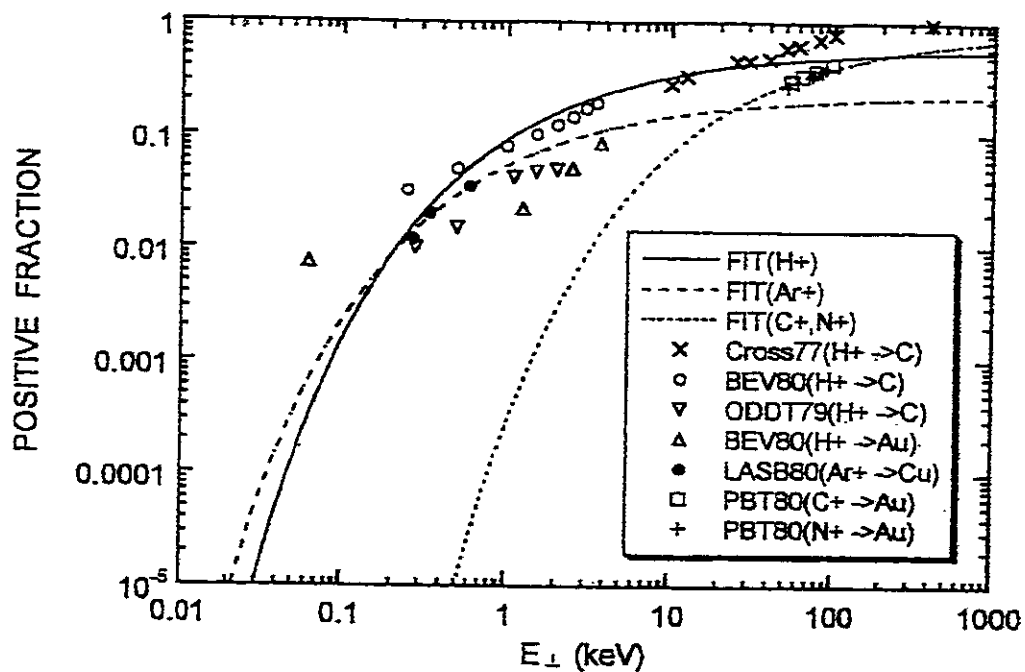

SEE or Y$^+$

BIAS (V)

Fig. 5. Charged fraction used in evaluation of the correction Y_c for secondary positive ion yield. Data are taken from refs. 11-15.
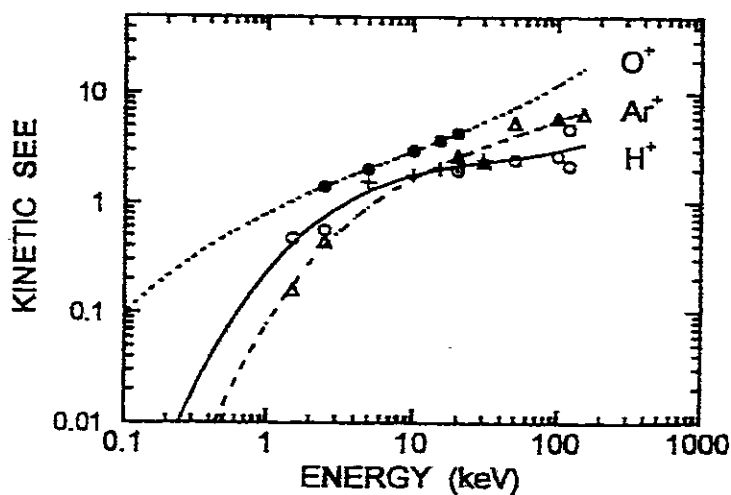

Fig. 6 Kinetic SEE from SUS or Fe: H^+(solid line), Ar^+(dashed line) and O^+(dotted line). Data for H^+(+) and O^+(●) are taken from ref. 16. Other data are measured in this study.

Recent Issues of NIFS-DATA Series

NIFS-DATA-45 Y. Yamamura, W Takeuchi and T Kawamura
The Screening Length of Interatomic Potential in Atomic Collisions: Mar 1998

NIFS-DATA-46 T Kenmotsu, T. Kawamura, T. Ono and Y Yamamura,
Dynamical Simulation for Sputtering of B4C Mar 1998

NIFS-DATA-47 I Murakami, K. Moribayashi and T. Kato,
Effect of Recombination Processes on FeXXIII Line Intensities May 1998

NIFS-DATA-48 Zhijie Li, T. Kenmotsu, T Kawamura, T Ono and Y Yamamura,
Sputtering Yield Calculations Using an Interatomic Potential with the Shell Effect and a New Local Model· Oct 1998

NIFS-DATA-49 S Sasaki, M Goto, T. Kato and S. Takamura,
Line Intensity Ratios of Helium Atom in an Ionizing Plasma: Oct. 1998

NIFS-DATA-50 I. Murakami, T. Kato and U Safronova,
Spectral Line Intensities of NeVII for Non-equilibrium Ionization Plasma Including Dielectronic Recombination Processses: Jan.
1999

NIFS-DATA-51 Hiro Tawara and Masa Kato,
Electron Impact Ionization Data for Atoms and Ions -up-dated in 1998- Feb 1999

NIFS-DATA-52 J G Wang, T. Kato and I Murakami,
Validity of n^{-3} Scaling Law in Dielectronic Recombination Processes: Apr. 1999

NIFS-DATA-53 J G. Wang, T. Kato and I Murakami,
Dielectronic Recombination Rate Coefficients to Excited States of He from He^+ Apr 1999

NIFS-DATA-54 T Kato and E. Asano,
Comparison of Recombination Rate Coefficients Given by Empirical Formulas for Ions from Hydrogen through Nickel: June 1999

NIFS-DATA-55 H P Summers, H Anderson, T Kato and S. Murakami,
Hydrogen Beam Stopping and Beam Emission Data for LHD· Nov 1999

NIFS-DATA-56 S Born, N. Matsunami and H. Tawara,
A Simple Theoretical Approach to Determine Relative Ion Yield (RIY) in Glow Discharge Mass Spectrometry (GDMS): Jan. 2000

NIFS-DATA-57 T Ono, T Kawamura, T. Kenmotsu, Y Yamamura,
Simulation Study on Retention and Reflection from Tungsten Carbide under High Fluence of Helium Ions Aug 2000

NIFS-DATA-58 J G Wang, M Kato and T Kato,
Spectra of Neutral Carbon for Plasma Diagnostics. Oct 2000

NIFS-DATA-59 Yu. V. Ralchenko, R K Janev, T Kato, D V Fursa, I Bray and F.J. de Heer
Cross Section Database for Collision Processes of Helium Atom with Charged Particles.
I. Electron Impact Processes· Oct 2000

NIFS-DATA-60 U I. Safronova, C. Namba, W R Johnson, M S. Safronova,
Relativistic Many-Body Calculations of Energies for n = 3 States in Aluminiumlike Ions: Jan 2001

NIFS-DATA-61 U.I Safronova, C Namba, I Murakami, W.R Johnson and M S Safronova,
E1,E2, M1, and M2 Transitions in the Neon Isoelectronic Sequence Jan. 2001

NIFS-DATA-62 R K Janev, Yu V. Ralchenko, T Kenmotsu,
Unified Analytic Formula for Physical Sputtering Yield at Normal Ion Incidence Apr 2001

NIFS-DATA-63 Y Itikawa,
Bibliography on Electron Collisions with Molecules Rotational and Vibrational Excitations, 1980-2000 Apr 2001

NIFS-DATA-64 R K. Janev, J G Wang and T.Kato,
Cross Sections and Rate Coefficients for Charge Exchange Reactions of Protons with Hydrocarbon Molecules· May 2001

NIFS-DATA-65 T Kenmotsu, Y. Yamamura, T Ono and T. Kawamura,
A New Formula of the Energy Spectrum of Sputtered Atoms from a Target Material Bombarded with Light Ions at Normal Incidence·
May 2001

NIFS-DATA-66 I Murakami, U I Safronova and T Kato,
Dielectronic Recombination Rate Coefficients to Excited States of Be-like Oxygen· May 2001

NIFS-DATA-67 N. Matsunami, E Hatanaka, J Kondoh, H. Hosaka, K. Tsumori, H. Sakaue and H. Tawara,
Secondary Charged Particle Emission from Proton Conductive Oxides by Ion Impact, July 2001